

CERN-TH/2000-080
NORDITA-2000/29HE
hep-lat/0003020

O(2) SYMMETRY BREAKING VS. VORTEX LOOP PERCOLATION

K. Kajantie^{a,1}, M. Laine^{b,a,2}, T. Neuhaus^{c,d,3}, A. Rajantie^{e,4}, K. Rummukainen^{f,g,5}

^a*Dept. of Physics, P.O.Box 9, FIN-00014 Univ. of Helsinki, Finland*

^b*Theory Division, CERN, CH-1211 Geneva 23, Switzerland*

^c*Institut für Theoretische Physik E, RWTH Aachen, FRG*

^d*ZiF, Univ. Bielefeld, D-33615 Bielefeld, FRG*

^e*Centre for Theor. Physics, Univ. of Sussex, Brighton BN1 9QH, UK*

^f*NORDITA, Blegdamsvej 17, DK-2100 Copenhagen Ø, Denmark*

^g*Helsinki Inst. of Physics, P.O.Box 9, FIN-00014 Univ. of Helsinki, Finland*

Abstract

We study with lattice Monte Carlo simulations the relation of global O(2) symmetry breaking in three dimensions to the properties of a geometrically defined vortex loop network. We find that different definitions of constructing a network lead to different results even in the thermodynamic limit, and that with typical definitions the percolation transition does not coincide with the thermodynamic phase transition. These results show that geometrically defined percolation observables need not display universal properties related to the critical behaviour of the system, and do not in general survive in the field theory limit.

CERN-TH/2000-080
NORDITA-2000/29HE
March 2000

¹keijo.kajantie@helsinki.fi

²mikko.laine@cern.ch

³neuhaus@physik.rwth-aachen.de

⁴a.k.rajantie@sussex.ac.uk

⁵kari@nordita.dk

1 Introduction

In a classic work [1], Banks, Kogut and Myerson showed that the partition function of a particular three-dimensional (3d) spin model with global $O(2)$ symmetry, called the Villain model, can equivalently be represented as a partition function of a dual theory in which the spin configurations are integer-valued and sourceless and can therefore be represented as configurations of closed loops. Moreover, they suggested that at the transition point where the global $O(2)$ symmetry gets restored, infinitely long loops become important. The loops of the dual theory can be identified with vortex lines of the original theory, and therefore this result suggests that also in other theories that contain topological defects, they might play an important role in determining the properties of the phase transition. As a consequence, many problems in condensed matter physics and cosmology could be simplified by concentrating only on the vortex loop degrees of freedom (see, e.g., [2] and references therein).

In many cases, this intuitive picture can be realized in the precise sense that the vortex tension T defined as the energy per unit length of an isolated vortex vanishes at the transition point [3, 4, 5]. Near the transition point, vortex loops behave as world lines of particles in $2+1$ d, and one can then conjecture that they could be described with an effective scalar field of mass T [6, 7]. However, it is rather difficult to measure the tension T in practice [5, 8, 9], which limits the practical uses of this approach.

Therefore, one may seek for alternative ways of studying the vortex degrees of freedom. A seemingly natural approach is to decompose every spin configuration generated in a lattice Monte Carlo simulation into a number of closed vortex loops. The hope is then that the transition could be identified with a non-zero probability of finding vortex loops that extend through the whole system, a phenomenon which is often called percolation.

Percolation has been used to study phase transitions in various different theories. Examples of this in condensed matter physics include the 3d XY (or Heisenberg) model [10, 11, 12], and in cosmology the corresponding global $O(2)$ field theory [13], both assumed to represent some features of the gauged Ginzburg-Landau theory where the loops would be interpreted as Nielsen-Olesen vortices. In particle physics, a similar approach has been used to give a physical interpretation for the confinement phase transition in non-Abelian gauge theories [14] and to define an order parameter in the crossover regime of the electroweak theory [15].

Given the large range of physical applications for the percolation picture, it is important to check whether it really works. Experience from the Ising model where a different kind of percolation may occur, related to clusters instead of vortex loops, has shown [16] that one has to be quite careful with this interpretation (for a recent discussion, see [17]). In the present paper we study with high precision lattice Monte Carlo simulations the geometric properties of a properly defined vortex loop network near the thermodynamic phase transition in the XY model and show that in all of

the cases considered, the percolation point fails to coincide with the thermodynamic singularity. Nevertheless, a description in terms of vortex degrees of freedom can still be useful in many other contexts, if used with caution.

2 Model

The 3d XY model is defined by

$$Z_{\text{XY}} = \int_{-\pi}^{\pi} \prod_{\mathbf{x}} d\theta_{\mathbf{x}} \exp\left(\beta \sum_{\mathbf{x}} \sum_{i=1}^3 \cos(\theta_{\mathbf{x}+i} - \theta_{\mathbf{x}})\right). \quad (2.1)$$

It belongs to the same universality class as the Villain model where the original consideration involving vortex loop degrees of freedom was carried out [1]. However, it is computationally simpler, its critical properties are known very accurately, and it is more directly related to continuum field theories such as the Ginzburg-Landau model.

Let us recall that the only parameter point of the XY model corresponding to a continuum field theory is the 2nd order transition point at $\beta = \beta_c$. Thus for obtaining results free from lattice artifacts, one should focus on the vicinity of β_c . From the statistical mechanics point of view, this is the region where physical observables show universal critical behaviour.

3 Method

In order to analyse accurately the universal behaviour close to β_c , we shall employ the finite size scaling method [18]. We recall that the idea of the method is to first locate the infinite-volume critical point of the system. One then measures finite-volume values for various observables at that point, and determines from them the critical exponents.

We will here address particularly two questions:

1. Does the infinite-volume extrapolation of the percolation critical point coincide with the thermodynamic critical point?
2. Sitting at the thermodynamic critical point, do percolation related observables show critical behaviour? If so, do the critical exponents match any of the known thermodynamic ones?

As a benchmark with which to compare, let us recall the known thermodynamic properties of scalar models with global $O(2)$ symmetry. In the XY case, the infinite volume critical point is at [19]

$$\beta_c = 0.454165(4). \quad (3.1)$$

Let us denote

$$E = - \sum_{\mathbf{x}} \sum_{i=1}^3 \cos(\theta_{\mathbf{x}+\mathbf{i}} - \theta_{\mathbf{x}}), \quad M = \sum_{\mathbf{x}} \cos(\theta_{\mathbf{x}}), \quad (3.2)$$

where we have assumed the symmetry breaking direction to be $\theta = 0$. For any operator O_i , one can define the related susceptibility,

$$C_i = N^3 \langle (O_i - \langle O_i \rangle)^2 \rangle, \quad (3.3)$$

where N^3 is the volume of the system. For energy (E) and magnetization (M) like observables at β_c , the susceptibilities diverge as

$$C_E \propto N^{\alpha/\nu}, \quad C_M \propto N^{\gamma/\nu}. \quad (3.4)$$

Here ν is the correlation length critical exponent. Magnetization itself scales at the critical point according to

$$\langle |M| \rangle \propto N^{-\beta/\nu}. \quad (3.5)$$

Finally, corrections to scaling are determined by an universal exponent ω ; for instance, the finite volume apparent critical point determined from C_E is assumed to behave as

$$\beta_c^N - \beta_c^{N=\infty} = c_1 \frac{1}{N^{1/\nu}} + c_2 \frac{1}{N^{1/\nu+\omega}} + \dots \quad (3.6)$$

The known results for the exponents appearing here are [19, 20, 21]:

α	β	γ	ν	ω	α/ν	β/ν	γ/ν
-0.01	0.35	1.32	0.67	0.79	-0.015	0.52	1.97

(3.7)

4 Observables

In order to locate the vortices in a given field configuration, we first define

$$Y_{i,\mathbf{x}} = [\theta_{\mathbf{x}+\mathbf{i}} - \theta_{\mathbf{x}}]_{\pi}, \quad (4.1)$$

where $[...]_{\pi}$ means $(...) \bmod 2\pi$ with a result in the interval $(-\pi, \pi]$. The winding number of a plaquette is then defined as

$$n_{ij,\mathbf{x}} = \frac{1}{2\pi} (Y_{i,\mathbf{x}} + Y_{j,\mathbf{x}+\mathbf{i}} - Y_{i,\mathbf{x}+\mathbf{j}} - Y_{j,\mathbf{x}}). \quad (4.2)$$

The simplest vortex-related quantity is now [22]

$$\langle O_{\text{tot}} \rangle = \langle |n_{ij,\mathbf{x}}| \rangle. \quad (4.3)$$

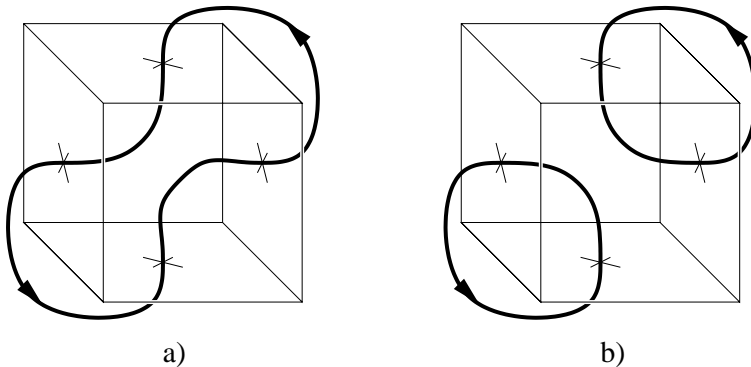


Figure 1: If two vortices pass through one cell, the vortex tracing algorithm must decide how to connect them, and this leads to an ambiguity in the length distribution.

It has the interpretation of the total vortex density, independent of their length. It is a perfectly well defined local observable, and any singularities in its finite volume behaviour are expected to be related to the thermodynamic singularities of the system.

However, in the continuum limit ($t = \beta - \beta_c \rightarrow 0$) O_{tot} smoothly approaches a constant value ≈ 0.160 , and the interpretation of O_{tot} as a vortex density becomes problematic: if we rescale the length scale by the physical correlation length $\xi \sim t^{-\nu}$, the vortex density diverges as $t^{-2\nu}$. From the continuum physics point of view, the density of vortex lines increases as we increase the resolution at which we look at the system, and finally we are measuring only ultraviolet fluctuations. This implies that quantities like the number of vortex loops and the length of individual loops are not well defined. The same problem arises also in more general continuum theories (see [23] and references therein).

These problems might be circumvented if we only monitor sufficiently long loops. Thus, we next connect single plaquettes with $n_{ij,x} \neq 0$ to a macroscopic closed vortex loop. This step involves a lot of ambiguity, see Fig. 1. We will employ two different “connectivity” definitions here:

- I. In the *maximal* definition, in each ambiguous case we make the unique choice so that the separate vortex loops are joined together, see Fig. 1.a.
- II. In the *stochastic* definition, in each ambiguous case the choice is made by throwing a dice. This is the procedure most commonly followed in the literature.

We can thus extract from each lattice configuration a set of “vortex loops”, consisting of a number of plaquettes which have been bound together by one of the connectivity definitions above. From this set of loops, we measure (using always cubic volumes N^3) the following observables:

1. “Closed loop order parameter”, O_{closed} . For a given configuration, $O_{\text{closed}} = 1$ if there is a vortex which forms a closed *non-contractible* loop around the lattice with periodic boundary conditions (in fact, there have to be at least two such loops, because the total topological charge is zero), and $O_{\text{closed}} = 0$ otherwise. We observe that $\langle O_{\text{closed}} \rangle$ approaches a step-like function at $N \rightarrow \infty$, being non-zero in the symmetric phase of the XY model. We can also consider a variant of this observable in which we count all vortices that extend over a distance $\geq N$ in any direction (O_{xyz}) or in some particular direction (O_x).

2. “Volume”, O_{vol} . We fit each vortex loop to the smallest possible rectangular box $n_1 \times n_2 \times n_3$. Let O_{vol} be the volume of the largest box compared with the total, $O_{\text{vol}} = n_1 n_2 n_3 / N^3$. We again observe that $\langle O_{\text{vol}} \rangle$ approaches a step function in the infinite-volume limit.

3. “Mass”, O_{mass} . For each configuration, we count the number of plaquettes visited by the longest loop L_0 , and normalise by the volume: $O_{\text{mass}} = (1/N^3) \sum_{\text{plaq.} \in L_0}$. We observe a vanishing result in the broken phase for $N \rightarrow \infty$, a non-vanishing in the symmetric phase, but a continuous behaviour at β_c . Thus $\langle O_{\text{mass}} \rangle$ behaves like the magnetization M but with an “inverted” β -axis.

4. “Line tension”, T_L . If in the idealised case of non-interacting loops, the tension, i.e. the mass per unit length, of a vortex is T , then the loop length distribution $\rho(L)$ has the form [12]

$$\rho(L) \sim L^{-5/2} \exp(-LT). \quad (4.4)$$

In the interacting case, the line tension T_L is defined by fitting the loop distribution $\rho(L)$ to a similar function,

$$\rho(L) \sim L^{-\alpha} \exp(-LT_L), \quad (4.5)$$

where α and T_L are free parameters. However, in the interacting case T_L should not be confused with the tension T given by the free energy per unit length of an isolated vortex. We observe that the line tension behaves similarly to the real (not the inverted) magnetization M .

For any observable O_i , $i = \{\text{closed}, xyz, x, \text{vol}, \text{mass}\}$, we define the percolation point β_i as the point where $\langle O_i \rangle$ vanishes when β is increased. Because of the similarities in the definitions of the observables, we expect there to be certain inequalities. Even in a finite system and in any configuration, the observables satisfy $O_{xyz} \geq O_{\text{closed}}$, $O_{xyz} \geq O_x$, as well as $O_{\text{vol}} \geq O_{\text{mass}}/3$ because each lattice cube has three plaquettes. The lattice symmetry also implies that $\langle O_x \rangle \geq \langle O_{xyz} \rangle/3$, because on the average at least every third long loop has to extend into the x -direction. These relations imply

$$\beta_{\text{mass}} \leq \beta_{\text{vol}}, \quad \beta_{\text{closed}} \leq \beta_{xyz} = \beta_x. \quad (4.6)$$

It also seems very plausible that in the infinite-volume limit, almost all configurations have either $O_{\text{vol}} = 0$ or 1 and consequently $O_{xyz} \geq O_{\text{vol}}$. We may also conjecture that in the infinite volume limit $\langle O_{\text{vol}} \rangle = \langle O_{xyz} \rangle$, and that $\langle O_{\text{mass}} \rangle > 0$ implies $\langle O_{\text{closed}} \rangle > 0$

because long volume filling loops have a finite probability to close. Therefore, we may expect that

$$\beta_{\text{mass}} \leq \beta_{\text{closed}} \leq \beta_{\text{vol}} = \beta_{xyz} = \beta_x, \quad (4.7)$$

and we cannot rule out the possibility that all these points are equal. However, in our actual analysis we only rely on Eq. (4.6), and use Eq. (4.7) just as a guidance.

5 Results

We have carried out simulations using both Swendsen-Wang and Wolff cluster algorithms. We use volumes in the range $4^3 \dots 200^3$. Individual runs have up to $\sim 10^6$ measurements at smaller volumes, $\sim 10^4$ at the largest ones.

5.1 Calibration

As a calibration of our accuracy we first briefly discuss the thermodynamic critical properties of the XY model, and show that we can reproduce the known results with good precision.

As an example, we show C_{tot} in Fig. 2(a) (cf. Eqs. (3.3), (4.3)). The critical point, defined as the point where C_{tot} obtains its maximum, is fit at relatively small volumes $4^3 \dots 48^3$ according to Eq. (3.6), with exponents fixed according to Eq. (3.7). We obtain $\beta_c = 0.45430(27)$, $\chi^2/\text{dof} = 0.19$, in agreement with Eq. (3.1). We can also leave both ν and ω as free parameters in the fit, but then the errors become quite large: $\nu = 0.83(15)$, $\omega = 1.16(42)$, $\beta_c = 0.45389(62)$, $\chi^2/\text{dof} = 0.16$. However, they are consistent with the values in Eqs. (3.1), (3.7). As another example, we sit precisely at the β_c given in Eq. (3.1), and measure the finite volume behaviour of magnetization with volumes $20^3 \dots 200^3$. We find the exponent $\beta/\nu = 0.5192(15)$, in agreement with Eq. (3.7). We conclude that our lattice sizes and statistics are sufficient to resolve the physical critical properties of the XY model.

5.2 Volume order parameter

We now move to our actual topic: percolation related observables. As an illustration of a behaviour similar to but not identical with that in Fig. 2(a), we first discuss the volume order parameter O_{vol} , determine its percolation critical point β_{vol} , and compare it with β_c in Eq. (3.1).

In Figs. 2(b),(c) we show the susceptibility C_{vol} , as well as its maximum position, measured with both types of connectivity definitions. We make an infinite volume fit according to Eq. (3.6), with exponents fixed as above, and another one with two free exponents. With the maximal connectivity definition we obtain

$$\beta_{\text{vol}} = 0.46184(14), \quad \nu = 0.67, \quad \omega = 0.79, \quad \chi^2/\text{dof} = 2.35, \quad (5.1)$$

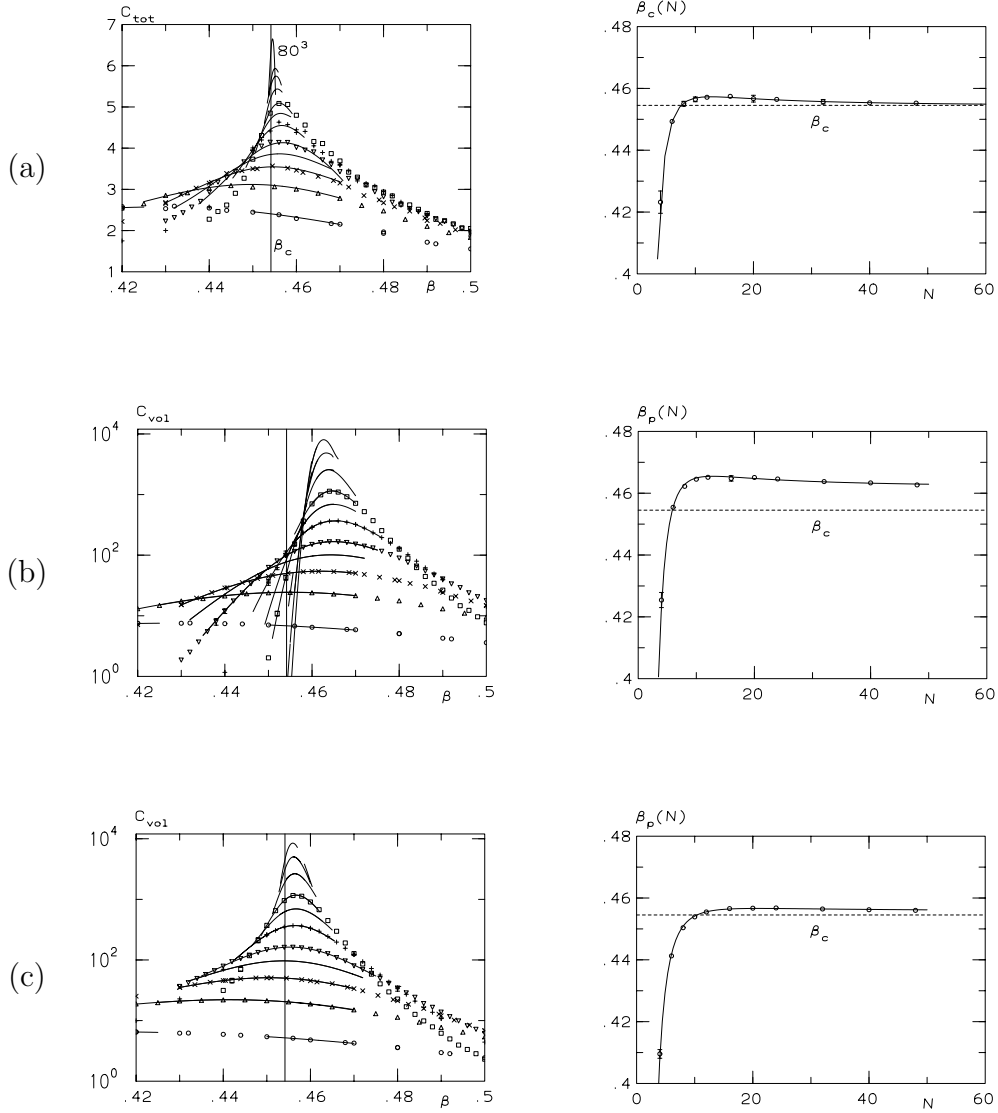


Figure 2: Left: different susceptibilities, Eq. (3.3), as a function of β ; (a) C_{tot} , (b) C_{vol} with the maximal connectivity definition, (c) C_{vol} with the stochastic connectivity definition. Right: the location of the apparent critical point determined from the maximum of C . The lines indicate the location of β_c .

$$\beta_{\text{vol}} = 0.46074(48), \quad \nu = 0.66(3), \quad \omega = 0.12(3), \quad \chi^2/\text{dof} = 0.64, \quad (5.2)$$

and with the stochastic definition

$$\beta_{\text{vol}} = 0.45565(13), \quad \nu = 0.67, \quad \omega = 0.79, \quad \chi^2/\text{dof} = 1.25, \quad (5.3)$$

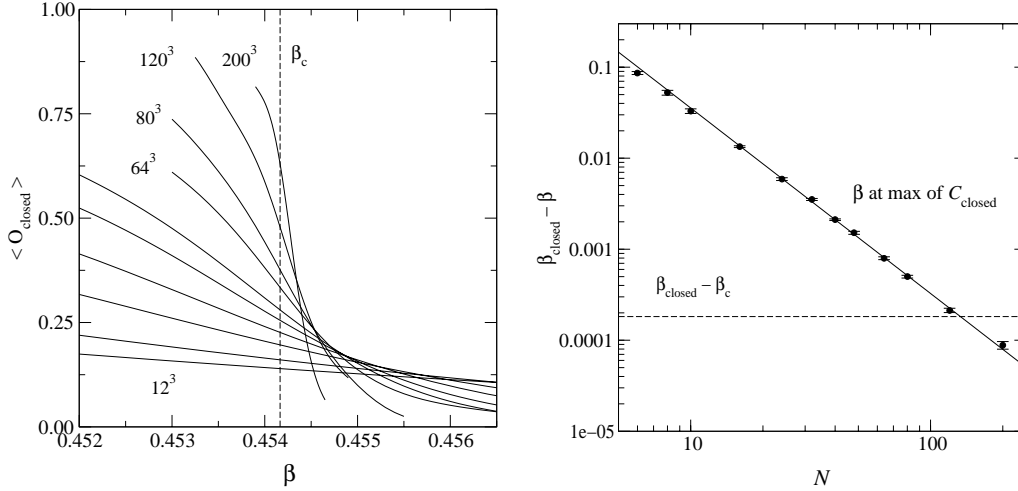


Figure 3: Left: the reweighted $\langle O_{\text{closed}} \rangle$ as a function of β . Right: the apparent percolation point as obtained from the position of the maximum of C_{closed} (or, for an observable only having values 0, 1, from the point where $\langle O_{\text{closed}} \rangle = 0.5$), together with the fit in Eq. (5.5) whereby $\beta_{\text{closed}} = 0.45435$. The log-log plot shows clearly that the power law describes the data well and $\beta_{\text{closed}} > \beta_c$ for $N \rightarrow \infty$.

$$\beta_{\text{vol}} = 0.45485(37), \quad \nu = 0.77(8), \quad \omega = 0.66(19), \quad \chi^2/\text{dof} = 0.07. \quad (5.4)$$

We observe that the location of β_{vol} depends on the definition used in constructing macroscopic vortex loops in a statistically significant way. The ambiguity inherent in this procedure is due to discretization (lattice) effects, cf. Fig. 1. Moreover, for the maximal connectivity definition, the percolation critical point is $\beta_{\text{vol}} \sim 0.461(1)$, far above the thermodynamic critical point, as is already apparent in Fig. 2. Even for the stochastic connectivity definition, β_{vol} does not coincide with the β_c , with a difference on the level of $(2\dots 3)\sigma$ depending slightly on the ansatz used for the $N \rightarrow \infty$ extrapolation. For a more precise statement we rely below on Eq. (4.6) and β_{mass} .

5.3 Closed loop order parameter

Consider then O_{closed} . As conjectured by Eq. (4.7), β_{closed} can be even closer to β_c than β_{vol} , and we have therefore carried out a more precise analysis with volumes up to 200^3 . The behaviour is shown in Fig. 3. A fit according to Eq. (3.6) to volumes $\geq 16^3$ with one free exponent gives

$$\beta_{\text{closed}} = 0.45435(3), \quad \nu = 0.490(6), \quad \chi^2/\text{dof} = 9.5/8. \quad (5.5)$$

The data is not accurate enough to allow for a good fit with two free exponents. A fit with exponents fixed to the thermodynamic values of ν and ω has $\chi^2/\text{dof} = 53/9$, and thus a very bad confidence level $\sim 2 \times 10^{-8}$.

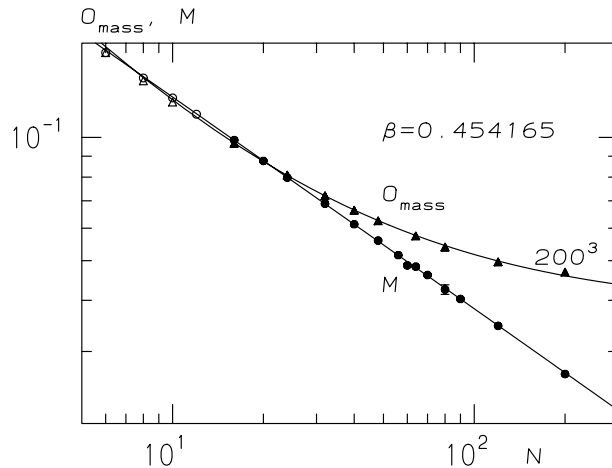


Figure 4: The behaviour of $\langle O_{\text{mass}} \rangle$ at β_c , compared with the thermodynamic quantity M defined in Eq. (3.2) (more precisely, $M/4$ in order to have similar magnitudes).

The central value of β_{closed} in Eq. (5.5) is now much closer to β_c than in Eq. (5.4). However the errors are also an order of magnitude smaller, due to the larger volumes used and the smaller range of reweighting in β . Thus the discrepancy is $\sim 6\sigma$. The disagreement can be very clearly seen in Fig. 3(right).

We do not consider separately the case of maximal connectivity, since it would increase β_{closed} moving it further away from β_c . Likewise, Eq. (4.6) shows that β_x and β_{xyz} cannot coincide with β_c , either.

5.4 Mass order parameter

Since both β_{vol} and β_{closed} are above β_c , Eq. (4.7) suggests that β_{mass} may be very close to it. A direct determination of β_{mass} is difficult because it turns out that there is no clear peak in C_{mass} up to very large volumes, due to strong fluctuations in the symmetric phase, and thus it is not easy to obtain finite volume estimates for β_{mass} . Therefore, we use a different technique to demonstrate that $\beta_{\text{mass}} > \beta_c$.

We stay precisely at β_c , given in Eq. (3.1) and measure $\langle O_{\text{mass}} \rangle$ on lattices of sizes up to 200^3 . The results are shown in Fig. 4. Recall that we expect a vanishing result at β_{mass} , and a finite value in the percolated phase $\beta < \beta_{\text{mass}}$. Since $\langle O_{\text{mass}} \rangle$ behaves similarly to magnetization with an inverted β -axis, we also show the magnetization in the same figure.

A fit to volumes $20^3 \dots 200^3$ with a single free exponent gives $0.60/N^{0.61(4)} + 0.0393(7)$, with $\chi^2/\text{dof} = 7.3/5$. This clearly shows a non-vanishing value in the thermodynamic limit. For the magnetization, a fit with a free exponent with volumes $20^3 \dots 200^3$ gives $1.1/N^{0.510(9)} - 0.002(3)$, $\chi^2/\text{dof} = 0.49$, consistent with $\beta/\nu = 0.52$ in Eq. (3.7) and a

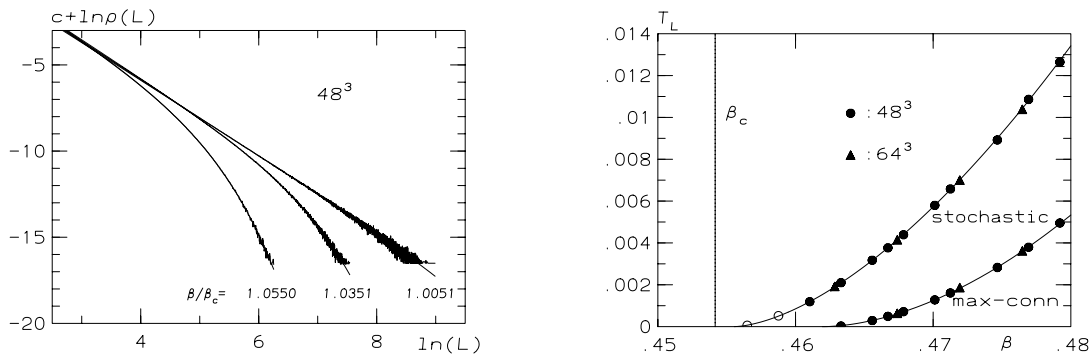


Figure 5: Left: The length distribution of vortices at β slightly above β_c with the stochastic definition. Right: the line tension, determined from the fit in Eq. (4.5) with a free parameter α , with both definitions.

vanishing result at $N \rightarrow \infty$. Thus, while magnetization exhibits the expected critical behaviour, from the point of view of O_{mass} we are already in the percolated phase, showing that $\beta_{\text{mass}} > \beta_c$. In the light of Eq. (4.6), this also confirms that $\beta_{\text{vol}} > \beta_c$.

5.5 Line tension

Let us finally discuss the line tension. The data is shown in Fig. 5. Since the analysis of T_L requires simulations at several values of $\beta > \beta_c$, we have performed the analysis using volumes 48^3 and 64^3 only. We will again monitor β_{T_L} , as well as a critical exponent γ_{T_L} , defined by

$$T_L \propto |\beta - \beta_{T_L}|^{\gamma_{T_L}}. \quad (5.6)$$

Since this behaviour assumes the infinite volume case, we cannot in practice go too close to β_c where the finite volume cuts off the critical fluctuations. At the same time, we should be close enough to β_c to be in the critical regime. In practice, we have chosen the window $\beta \in (0.46, 0.48)$ to satisfy these requirements, and have checked the volume independence at a couple of β , see Fig. 5(right).

Using the stochastic definition, a fit to Eq. (4.5) in this range gives $\alpha = 2.11(2)$, and T_L as shown in Fig. 5(right). Fitting this T_L to Eq. (5.6), as well as the one obtained with a fixed $\alpha = 2.5$, we get

$$\alpha = 2.11(2), \quad \beta_{T_L} = 0.4555(2), \quad \gamma_{T_L} = 1.62(3), \quad \chi^2/\text{dof} = 0.27, \quad (5.7)$$

$$\alpha = 2.5, \quad \beta_{T_L} = 0.4558(4), \quad \gamma_{T_L} = 1.67(5), \quad \chi^2/\text{dof} = 2.7. \quad (5.8)$$

If β_{T_L} is fixed by hand to a smaller value, γ_{T_L} can go up to ~ 1.72 . The maximal connectivity definition gives clearly contradicting numbers, see Fig. 5(right), with an

exponent $\gamma_{T_L} = 1.80(3)$.

In conclusion, the percolation point β_{T_L} again differs significantly from the critical point in Eq. (3.1). Moreover, the values we find for γ_{T_L} do not coincide with any of the thermodynamic exponents.⁶

6 Conclusions

It is quite obvious that in discrete spin models even naive geometrically defined percolation observables show structure close to the thermodynamic phase transition. Indeed, the ordered and disordered phases of the spin models are quite well understood, and either almost frozen (in the ordered phase), or with almost random fluctuations (in the disordered phase), which guarantees that percolation seems to take place. The question we have addressed here is whether this rough agreement can be promoted to a precise level in the vicinity of the thermodynamic transition point, where the spin models show universal critical behaviour, and allow to define a non-trivial continuum field theory.

We have found that in the three-dimensional XY model, the geometrically defined percolation transition of the vortex loops is extremely close to the thermodynamic phase transition, but does not coincide with it with any of the observables we have used. There is a clear discrepancy between the “maximal” and “stochastic” definitions used for constructing macroscopic vortex loops. Even with the stochastic definition, a finite-size scaling analysis at the thermodynamic critical point, whose location is known very accurately from previous studies, shows the absence of any true critical behaviour. We of course cannot exclude that it would be possible to bring the percolation transition even closer to the thermodynamic one by very carefully fine-tuning the percolation criteria; however, this kind of a procedure would have no predictive power.

We believe that these conclusions apply also to more realistic theories, such as the Ginzburg-Landau theory of superconductivity and non-Abelian gauge theories. These theories are typically much more complicated than the XY model used here, and therefore it is in most cases very difficult to achieve the level of accuracy needed to confirm this in a Monte Carlo simulation. However, we may note that the observation of a percolation transition related to so called Z -vortices in crossover regime of the electroweak theory [15] bears a similarity with our conclusion.

Finally, we would like to emphasise that although geometrically defined percolation observables may not reflect the properties of the true phase transition in a rigorous sense, the description of the system in terms of the vortex loop degrees of freedom can still be useful, if a good observable is chosen. This is certainly true for the tension T

⁶Our result for the exponent γ_{T_L} does not agree with $\gamma_{T_L} = 1.45(5)$ measured in [12], nor with $\gamma_{T_L} = 1.50(1)$ measured in [13]. However, the fitted β ranges there were about 10 [12] or more [13] times wider than in our case, so that corrections to asymptotic scaling could play a role.

as discussed in the Introduction, and might also be the case in the non-equilibrium dynamics well after a cosmological phase transition, when the vortex loops cease to be merely thermal fluctuations and become macroscopic classical objects [24].

Acknowledgements

The simulations were carried out with a number of workstations at the Helsinki Institute of Physics and at Nordita, as well as with an Origin 2000 at the Center for Scientific Computing, Finland. This work was partly supported by the TMR network *Finite Temperature Phase Transitions in Particle Physics*, EU contract no. FMRX-CT97-0122. T.N. acknowledges support from DFG and discussion with H. Kleinert, and A.R. was partly supported by the University of Helsinki.

References

- [1] T. Banks, R. Myerson and J. Kogut, Nucl. Phys. B 129 (1977) 493.
- [2] G.A. Williams, Phys. Rev. Lett. 82 (1999) 1201 [cond-mat/9807338].
- [3] G. 't Hooft, Nucl. Phys. B 138 (1978) 1; Nucl. Phys. B 153 (1979) 141.
- [4] G. Di Cecio, A. Di Giacomo, G. Paffuti and M. Trigiane, Nucl. Phys. B (Proc. Suppl.) 53 (1997) 584 [hep-lat/9608014].
- [5] K. Kajantie, M. Laine, T. Neuhaus, J. Peisa, A. Rajantie and K. Rummukainen, Nucl. Phys. B 546 (1999) 351 [hep-ph/9809334].
- [6] A. Kovner, B. Rosenstein and D. Eliezer, Nucl. Phys. B 350 (1991) 325; A. Kovner, P. Kurzepa and B. Rosenstein, Mod. Phys. Lett. A 8 (1993) 1343 [hep-th/9303144].
- [7] M. Kiometzis, H. Kleinert and A.M.J. Schakel, Fortschr. Phys. 43 (1995) 697 [cond-mat/9508142].
- [8] T.G. Kovacs and E.T. Tomboulis, hep-lat/0002004.
- [9] K. Kajantie, M. Laine, T. Neuhaus, A. Rajantie and K. Rummukainen, Nucl. Phys. B 559 (1999) 395 [hep-lat/9906028].
- [10] A.V. Pochinsky, M.I. Polikarpov and B.N. Yurchenko, Phys. Lett. A 154 (1991) 194.
- [11] A. Hulsebos, hep-lat/9406016.
- [12] A.K. Nguyen and A. Sudbø, Phys. Rev. B 60 (1999) 15307 [cond-mat/9907385].

- [13] N.D. Antunes, L.M. Bettencourt and M. Hindmarsh, Phys. Rev. Lett. 80 (1998) 908 [hep-ph/9708215]; N.D. Antunes and L.M. Bettencourt, Phys. Rev. Lett. 81 (1998) 3083 [hep-ph/9807248].
- [14] M. Engelhardt, K. Langfeld, H. Reinhardt and O. Tennert, Phys. Rev. D 61 (2000) 054504 [hep-lat/9904004].
- [15] M.N. Chernodub, F.V. Gubarev, E.-M. Ilgenfritz and A. Schiller, Phys. Lett. B 443 (1998) 244 [hep-lat/9807016].
- [16] H. Müller-Krumbhaar, Phys. Lett. A 50 (1974) 27.
- [17] S. Fortunato and H. Satz, hep-lat/9911020.
- [18] M.N. Barber, in *Phase Transition and Critical Phenomena*, Vol. 8, eds. C. Domb and J.L. Lebowitz (Academic Press, London, 1983).
- [19] H.G. Ballesteros, L.A. Fernández, V. Martin-Mayor and A. Muñoz Sudupe, Phys. Lett. B 387 (1996) 125 [cond-mat/9606203].
- [20] J. Zinn-Justin, *Quantum Field Theory and Critical Phenomena*, 2nd ed. (Oxford University Press, Oxford, 1993).
- [21] A.P. Gottlob and M. Hasenbusch, Physica A 201 (1993) 593.
- [22] G. Kohring, R.E. Shrock and P. Wills, Phys. Rev. Lett. 57 (1986) 1358.
- [23] K. Kajantie, M. Karjalainen, M. Laine, J. Peisa and A. Rajantie, Phys. Lett. B 428 (1998) 334 [hep-ph/9803367].
- [24] M.B. Hindmarsh and T.W.B. Kibble, Rep. Prog. Phys. 58 (1995) 477; A. Vilenkin and E.P.S. Shellard, *Cosmic Strings and other Topological Defects* (Cambridge University Press, Cambridge, 1994).